Wave effects on hinged bodies
Part I – body motions

J. N. NEWMAN

December 9, 1997

1 INTRODUCTION

WAMIT can be used with appropriate generalized modes to describe the coupled motions of an ensemble of separate floating bodies connected by hinges, as well as structural loads and deflections of each body. The theoretical background for this analysis is presented in [1]. To illustrate the methodology we shall consider a longitudinal array of N identical rigid modules connected by frictionless hinges.

Following the convention in WAMIT a Cartesian coordinate system x, y, z is used with $z = 0$ the undisturbed free surface, x positive toward the 'bow' of the array, y positive toward the port side of the array, and z positive upwards. Each module is considered to be a floating vessel with geometric symmetry about the vertical centerplane $y = 0$ and also about its midship section. The origin $x = 0$ is at the midpoint of the array. Simple transverse hinge joints are located at $x = x_n$ $(n = 1, 2, ..., N - 1)$. These are numbered in ascending order from the stern to the bow. The overall length L of each module is defined as the distance between adjacent hinges, $x_{n+1} - x_n$.

In general the motions of the array will include six conventional modes (surge, sway, heave, roll, pitch, yaw) where the entire array is translating and rotating as a rigid body, and $N-1$ additional 'generalized' modes corresponding to deflections of the hinges. The analysis of the rigid-body motions is classical, and our main concern here is to extend the computational procedure to include the hinge-deflection modes as well as any coupling that may exist with the six conventional modes. Since the array geometry is symmetric about $y = 0$, and the hinge axes are parallel to the y-axis, there is no coupling between the vertical motions considered here and the sway, roll, and yaw motions. Thus we shall ignore the latter three modes, which can be analysed independently from the hinge-deflection modes.

To simplify the following analysis we shall assume that the hinge axes are in the plane $z = 0$, and consider only the vertical motions of each module associated

with the modes of heave, pitch, and the hinge deflections. It is straightforward to consider the coupling with surge, and hinges which are located at other vertical positions.

Since we only consider heave and pitch, and the deflections of $N-1$ hinges, a total of $N+1$ degrees of freedom exist. Each degree of freedom can be described by an appropriate function $f_j(x)$ which describes the elevation due to motion with unit amplitude in each separate mode. In the time domain each mode is multiplied by a corresponding amplitude $a_j(t)$, and the total superposition of all the modes is

$$f(x,t) = \sum_{j=1}^{N+1} a_j(t) f_j(x) \tag{1.1}$$

In the frequency-domain description each spectral frequency ω is treated separately, and (1.1) can be rewritten in the form

$$f(x,t) = \text{Re}\left[e^{i\omega t} \sum_{j=1}^{N+1} \xi_j f_j(x) \right] \tag{1.2}$$

The response-amplitude operators ξ_j are complex, representing the amplitude and phase of each modal response at the frequency ω.

The definition and numbering of each mode is somewhat arbitrary, but the analysis is simplified if these are defined carefully at the outset. In WAMIT the indices $j = 1, 2, ..., 6$ are reserved for the six rigid-body motions, with $j = 3, 5$ corresponding to heave and pitch respectively. Additional 'generalized modes' are identified by consecutive indices $j = 7, 8, ...$ In the description below it is simpler to use a more compact numbering system, where heave and pitch are identified by $j = 1, 2$ and the additional hinge-deflection modes by $j = 3, 4, ..., N+1$. We shall define the latter modes initially conrresponding to unit elevation of each hinge ($n = 1, 2, ..., N-1$) with all other hinges at the static position $z = 0$. The generalized modes defined in this manner are neither symmetric/antisymmetric, nor orthonormal.

Since the geometry of the array is symmetrical about the planes $x = 0$ and $y = 0$, substantial reductions in computing time and memory can be achieved if the modes are defined to be either symmetric or antisymmetric about the same planes. In Section 2 we first consider the appropriate modes to use irrespective of symmetry, and then the alternative modes which separate all motions into their symmetric and antisymmetric components.

In addition to these 'hinge modes', appropriate generalized modes may be required to represent the structural deflection of each module, or simply to assist in the evaluation of the structural loads. A distinction is made here between (a) 'active' modes used in a 'hydroelastic' analysis where the structural deflections are significant, and (b) 'passive' modes which are used to evaluate the structural loads in the undeformed state. The hydroelastic analysis is not generally required unless the magnitude of the structural deflection is comparable to the other modes of motion and/or the incident-wave amplitude. The use of gener-

alized modes to evaluate the structural loads will be considered subsequently in Part 2.

2 GENERALIZED HINGE MODES

In defining the generalized modes it is convenient to normalize the longitudinal coordinate x relative to the length L. We use the nondimensional coordinate $u = x/L$, and define the modes as functions of u. The hinge axes are at $u = u_n = x_n/L$. If N is even, the hinges are at $u = 0, \pm 1, \pm 2, ...$, and if N is odd the hinges are at $\pm\frac{1}{2}, \pm\frac{3}{2}, ...$ In all cases the heave and pitch modes are defined by the vertical deflections $f_1 = 1$, $f_2 = -uL$. (The factor L is required in the latter case since the pitch mode is defined with vertical displacement $-x$ in the dimensional coordinate system.)

First consider the simplest case of two rigid bodies with one hinge at $u = 0$. The hinge mode will be defined in this case as $f_3(u) = 1 - |u|$, with unit displacement at the hinge and zero displacement at the ends. This mode is symmetric about $u = 0$. It is referred to as a 'tent function' due to its shape. For subsequent analysis it is convenient to define the function

$$t(u) = 1 - |u| \quad (0 < |u| < 1), \qquad t(u) = 0 \quad (|u| > 1) \tag{2.1}$$

The only generalized mode required for $N = 2$ is $f_3 = t(u)$, as shown in Figure 1.

Tent functions can be used more generally to represent the hinge deflections of an array with any number of modules. A complete set of modes which do not satisfy the symmetry/antisymmetry requirement are defined by

$$\hat{f}_j(u) = t(u - u_n) \qquad \begin{array}{l} (j = 3, 4, 5, ..., N + 1) \\ (n = 1, 2, 3, ..., N - 1) \end{array} \tag{2.2}$$

Each mode $\hat{f}_j$ corresponds to a triangular elevation of the two modules adjacent to the hinge $n = j - 2$, with no motion of the other modules.

Alternatively, an equivalent set of generalized modes can be defined such that they are either symmetric about $u = 0$ (j odd) or antisymmetric (j even). This is achieved by combining the tent functions as follows:

$$f_j(u) = t(u - u_n) + t(u - u_{N-n}) \qquad \begin{array}{l} (j = 3, 5, 7, ..., 2[\frac{N-1}{2}] + 1) \\ (n = 1, 2, 3, ..., [\frac{N-1}{2}]) \end{array}$$

$$f_{N+1}(u) = t(u - u_{N/2}) \qquad (N \text{ even}) \tag{2.3}$$

$$f_j(u) = t(u - u_n) - t(u - u_{N-n}) \qquad \begin{array}{l} (j = 4, 6, 8, ..., 2[\frac{N+1}{2}]) \\ (n = 1, 2, 3, ..., [\frac{N-1}{2}]) \end{array} \tag{2.4}$$

Here the symbol $[a]$ denotes the largest integer which is less than or equal to a. For N even there are a total of $N/2$ generalized symmetric modes and $N/2 - 1$ antisymmetric modes. The last symmetric mode is a single tent function at

the center hinge $u = u_{N/2} = 0$. For N odd there are $(N-1)/2$ generalized symmetric modes and the same number of antisymmetric modes. The last mode is $j = N+1$. These modes are illustrated in Figure 1 for $N = 1, 2, 3, 4, 5$.

The usual step in representing a general function $f(x)$ as a combination of symmetric and antisymmetric components is in terms of the sum and difference of the two separate functions, $[f(x) \pm f(-x)]$. In (2.3-4) we have implicitly used the facts that $t(u)$ is an even function, and $u_{N-n} = -u_n$, to replace $t(-u-u_n)$ by the more physical and equivalent function $t(u-u_{N-n})$.

Generalized moments will be defined by the integrals

$$I_{ij} = \int f_i(u) f_j(u) du \tag{2.5}$$

where the integration is over the complete array. The moments associated with the heave and pitch modes $f_1 = 1$, $f_2 = -x = -Lu$ are

$$\begin{aligned}
I_{11} &= N \\
I_{1j} &= 2 \quad (j = 3, 5, 7, ..., 2[\tfrac{N-1}{2}] + 1) \\
I_{1,N+1} &= 1 \quad (N \text{ even}) \\
I_{22} &= \tfrac{1}{12} N^3 L^2 \\
I_{2j} &= -L(u_n - u_{N-n}) \quad (n = \tfrac{1}{2} j - 1) \\
&= L(N - j + 2)
\end{aligned}$$

The other moments can be evaluated by substituting (2.3) or (2.4) in (2.5) and using the relations

$$\begin{aligned}
\int t(u-u_m)\, t(u-u_n) du &= \tfrac{2}{3} \quad (m = n) \\
&= \tfrac{1}{6} \quad |m-n| = 1 \\
&= 0 \quad |m-n| \geq 2
\end{aligned}$$

More explicit results are listed in Table 1. In all cases $I_{ij} = I_{ji}$, and $I_{ij} = 0$ if $(i+j)$ is odd.

With some additional algebra it is possible to systematically define an alternative set of symmetric/antisymmetric orthonormal modes $\tilde{f}_j(u)$ by superposition of the nonorthogonal modes (2.3-4). We define the orthonormal modes in the form

$$\begin{aligned}
\tilde{f}_i(u) &= \sum_{j=1}^{i} C_{ij} f_j(u) \qquad (i = 3, 5, 7, ..., 2[\tfrac{N}{2}] + 1) \\
\tilde{f}_i(u) &= \sum_{j=2}^{i} C_{ij} f_j(u) \qquad (i = 4, 6, 8, ..., 2[\tfrac{N+1}{2}])
\end{aligned} \tag{2.6}$$

where $C_{ij} = 0$ if $(i+j)$ is odd. The corresponding moments are

$$\tilde{I}_{ij} = \int \tilde{f}_i(u) \tilde{f}_j(u) du = \delta_{ij} \tag{2.7}$$

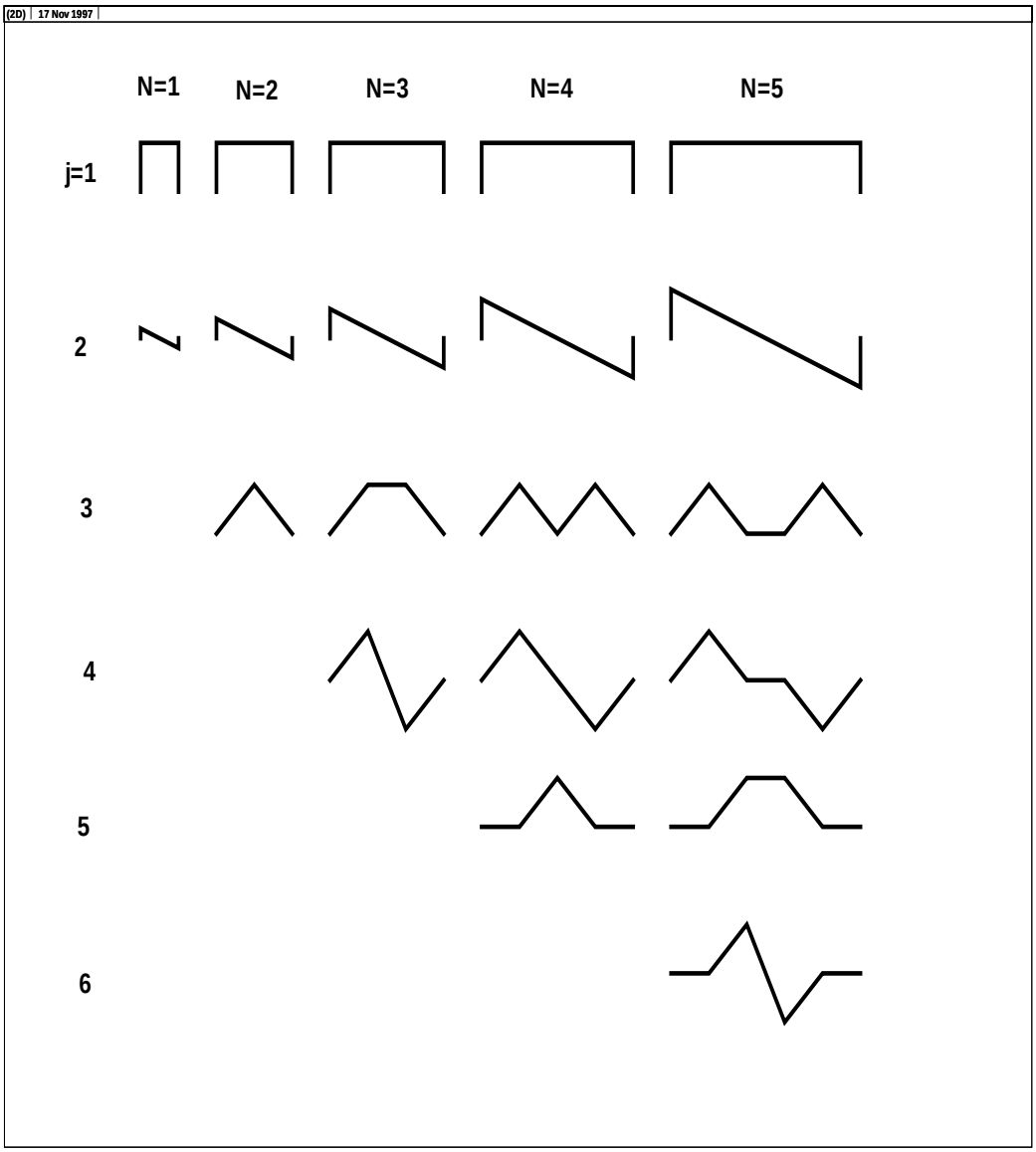

Figure 1: Symmetric and antisymmetric modes f_j used to represent the vertical motions of an array. The number of separate modules N is shown at the top of each column, and the mode index j is shown in the left column. The first two modes correspond to heave and pitch, followed by the hinge deflection modes (2.3-4). For pitch the scale is normalized by the module length L. Note that the index j used here differs from the WAMIT mode index, where the corresponding indices $j = 3, 5, 7, 8, 9, 10$ replace the values shown in column 1.

$\lvert m-n\rvert$	$\lvert N-m-n\rvert$	symmetric	antisymmetric
0	1	5/3	1
0	≥ 2	4/3	4/3
1	1	2/3	0
1	≥ 2	1/3	1/3
≥ 2	1	1/3	$-1/3$
≥ 2	≥ 2	0	0

Table 1: Values of I_{ij} for symmetric and antisymmetric modes $(i \geq 3)$ $(j \geq 3)$. The hinge indices are defined by $m = [\frac{i-1}{2}]$ and $n = [\frac{j-1}{2}]$.

where the Kroenecker delta function δ_{ij} is equal to 1 if $(i = j)$, and equal to zero if $(i \neq j)$. For each value of i the coefficients C_{ij} can be evaluated recursively by substituting (2.6) in (2.7), and solving a linear system of equations of dimension $[\frac{i+1}{2}]$. The coefficient matrix and right-hand-side vector involve the moments I_{ij}.

3 HYDRODYNAMIC SOLUTION

Time-harmonic motions of small amplitude are considered, with the complex factor $\mathrm{e}^{i\omega t}$ applied to all first-order oscillatory quantities. The boundary conditions on the body and free surface are linearized, and potential flow is assumed.

We follow the same notation as in [1], where a more complete statement of the problem is outlined. The fluid velocity field is represented by the gradient of the velocity potential $\mathrm{Re}\,\phi \mathrm{e}^{i\omega t}$, where $\phi(x, y, z)$ is a complex function governed by Laplace's equation in the fluid domain with appropriate boundary conditions on the free surface and bottom. The velocity potential of the incident wave is defined by

$$\phi_I = \frac{igA}{\omega} \frac{\cosh[k(z+h)]}{\cosh kh} e^{-ik(x\cos\beta + y\sin\beta)}, \tag{3.1}$$

where g is the gravitational acceleration, A the wave amplitude, the wavenumber k is the positive real root of the dispersion relation

$$\frac{\omega^2}{g} = k \tanh kh, \tag{3.2}$$

h is the fluid depth, and β is the angle between the direction of propagation of the incident wave and the positive $x-$axis. If the fluid depth is large compared to the characteristic wavelength $2\pi/k$ the infinite-depth limit can be used in place of (3.1):

$$\phi_I = \frac{igA}{\omega} e^{kz - ik(x\cos\beta + y\sin\beta)}, \tag{3.3}$$

where $\omega^2/g = k$.

The velocity potential ϕ can be expressed in the form

$$\phi = \phi_R + \phi_D, \tag{3.4}$$

where

$$\phi_D = \phi_I + \phi_S \tag{3.5}$$

is the diffraction potential, ϕ_S is the scattering component representing the disturbance of the incident wave by the fixed body, and

$$\phi_R = \sum_{j=1}^{J} \xi_j \phi_j \tag{3.6}$$

is the radiation potential due to the body's motions, with complex amplitude ξ_j in each mode. In each mode, ϕ_j is the corresponding unit-amplitude radiation potential.

On the undisturbed position of the body boundary, the radiation and diffraction potentials are subject to the conditions

$$\frac{\partial \phi_j}{\partial n} = i\omega n_j \tag{3.7}$$

$$\frac{\partial \phi_D}{\partial n} = 0. \tag{3.8}$$

Here n_j is the normal component of the displacement on the body surface, associated with mode j. For vertical displacements defined by the modes in Section 2, $n_j = f_j n_z$ where n_z is the vertical component of the unit normal vector on the body surface, defined pointing from the fluid into the body.

The boundary-value problem is completed by imposing a radiation condition of outgoing waves, for the potentials ϕ_S and ϕ_j.

Corresponding to each mode of motion, generalized first-order pressure forces are defined by appropriate weighted integrals of the pressure over the submerged surface S in the form

$$F_i = \iint_S p n_i dS = -\rho \iint_S \Big(i\omega\phi + gz \Big) n_i dS. \tag{3.9}$$

Here p is the fluid pressure, which is evaluated in the last form of (3.9) from the linearized Bernoulli equation.

After substituting (3.6) for the components of the radiation potential, added-mass and damping matrices are defined in the form

$$\omega^2 a_{ij} - i\omega b_{ij} = -i\omega\rho \iint_S \phi_j n_i dS \tag{3.10}$$

Similarly, the generalized wave-exciting force is

$$X_i = -i\omega\rho \iint_S \phi_D n_i dS \tag{3.11}$$

The indices i and j can take on any values within the ranges of the rigid-body modes (1-2) and extended modes (3,4,...).

For the case considered here where the only body motions are described by vertical displacements, the hydrostatic restoring matrix is defined by

$$c_{ij} = \rho g \iint_S f_i n_j dS = \rho g \iint_S f_i f_j n_z dS. \tag{3.12}$$

4 FREE MOTIONS OF THE ARRAY

Assuming each module to be rigid, equations of motion can be derived by equating the hydrodynamic pressure force coefficients in Section 3 to the corresponding inertial force coefficients M_{ij} for the internal mass distribution of the structure. For a single body which is free in the heave and pitch modes, appropriate equations of motion are derived by integrating the pressure force and its first moment along the length, and equating these to the corresponding inertial force and moment. More generally, for the array with hinged connectors and no external constraints, the same procedure is adopted including integrals along the length weighted by each mode function.

Proceeding in this manner, the inertial effects associated with the body mass are defined by the mass matrix

$$M_{ij} = \int m(x) f_i(x) f_j(x) dx \tag{4.1}$$

where the integration is over the entire array, and $m(x)$ is the longitudinal density of mass. Adding these coefficients to the corresponding added-mass coefficients the equations of motion are obtained in the form

$$\sum_{j=1}^{N+1} \xi_j \left[-\omega^2 (a_{ij} + M_{ij}) + i\omega b_{ij} + c_{ij} \right] = X_i \quad (i = 1, 2, 3, ..., N+1) \tag{4.2}$$

The summation on the left side of (4.2) is over all modes including heave, pitch, and the hinge deflections.

After solving the linear system of equations (4.2) for the $N+1$ unknown mode amplitudes ξ_j the motions of the array can be evaluated by modal superposition, with the results

$$\begin{aligned} f(x_n, t) &= \mathrm{Re}\left(\xi_1 - \xi_2 x_n + \xi_j + \xi_{j+1}\right) e^{i\omega t} \quad (n = 1, 2, ..., [\tfrac{N-1}{2}]), \\ &\qquad\qquad (j = 2n+1) \\ &= \mathrm{Re}\left(\xi_1 - \xi_2 x_n + \xi_j\right) e^{i\omega t} \qquad (n = \tfrac{N}{2}),\ (j = 2n+1) \\ &= \mathrm{Re}\left(\xi_1 - \xi_2 x_n + \xi_j - \xi_{j+1}\right) e^{i\omega t} \quad (n = [\tfrac{N+1}{2}], ..., N-1), \\ &\qquad\qquad (j = 2N - 2n + 1) \end{aligned} \tag{4.3}$$

Here the first and second term represent the vertical motions due to heave and pitch, and the last term(s) are the superposition of the symmetric and antisymmetric hinge modes.

5 ARRAY OF BARGES

To illustrate the methodology we shall describe computational results for an articulated rectangular barge with five sections. To simplify the details of the geometry near the hinges, the submerged surface is assumed to be continuous, with a total length $5L$, beam B, and draft T. To conform with the horizontal dimensions and displacement of typical MOB configurations these dimensioins are chosen to be 6000 feet, 500 feet, and 20 feet, respectively. The four hinges are at $x = x_n = (-1800,\ -600,\ 600,\ 1800)$ feet.

One quadrant ($x > 0,\ y > 0$) of the submerged surface is discretized with N_A panels in the longitudinal direction, N_B panels in the transverse direction, and N_C panels vertically on the side and end. The total number of panels, and unknowns, is $N_A \times N_B + N_A \times N_C + N_B \times N_C$. Uniform spacing is used in the longitudinal direction to facilitate subdivision at the hinges. Two discretizations are compared to indicate the convergence of the results.

In the first discretization we use $N_A = 100$, $N_B = 10$, $N_C = 2$, giving a total of 1220 panels on one quadrant, with uniform spacing in the transverse and vertical directions.. To verify convergence of the results a finer discretization is used with $N_A = 150$, $N_B = 12$, $N_C = 4$, giving 2448 panels on one quadrant, and using nonuniform transverse 'cosine' spacing near the bilge corners.

Wave periods from 6 to 30 seconds are considered, with wave heading angles $\beta = 0$, 30, and 60°. Infinite fluid depth is assumed.

The results in Figures 2-7 show the amplitudes of the vertical motions at the ends of each module, progressing from the stern to the bow with intermediate points at the four hinges. In each case the amplitude (RAO) is normalized by the incident wave elevation. These figures are based on computations using the first discretization, with half-second increments of the wave period. Analogous computations with the fine discretization have been performed at one-second increments; the two sets of results agree within a maximum absolute difference of 0.009.

In general, the vertical motions are small for wave periods below 10 seconds, whereas for periods of 25-30 seconds the RAO's approach their asymptotic values of unity for long wavelengths. Resonant peaks occur at intermediate wave periods between 15 and 25 seconds, with peak values of 1.2-1.4 aft of the center, increasing to 1.7 at hinge 4 and 2.2 at the bow.

References

[1] J. N. Newman, 'Wave effects on deformable bodies,' Applied Ocean Research, Volume 16 (1994).

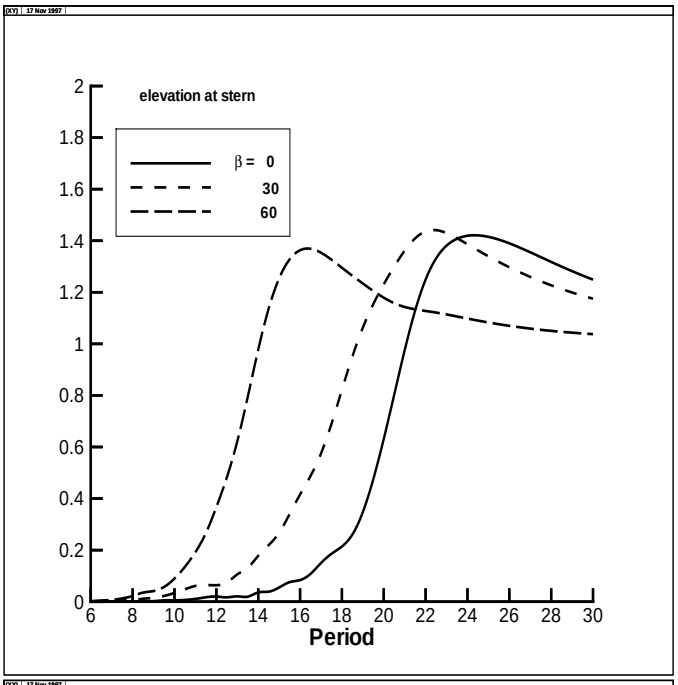

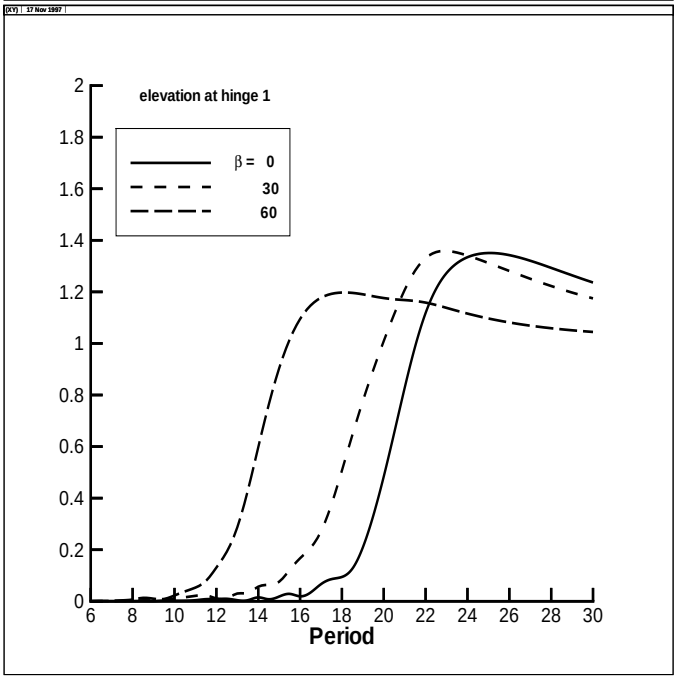

Figure 2: RAO's for stern and hinge 1.

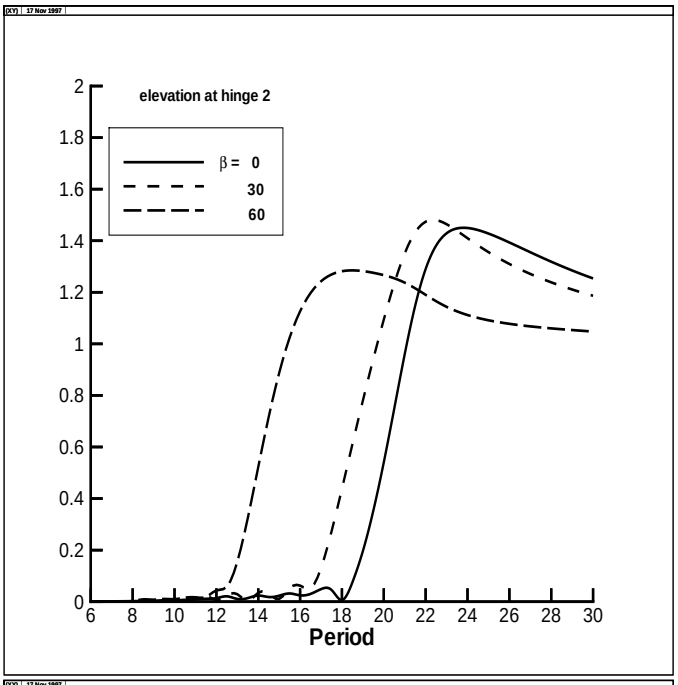

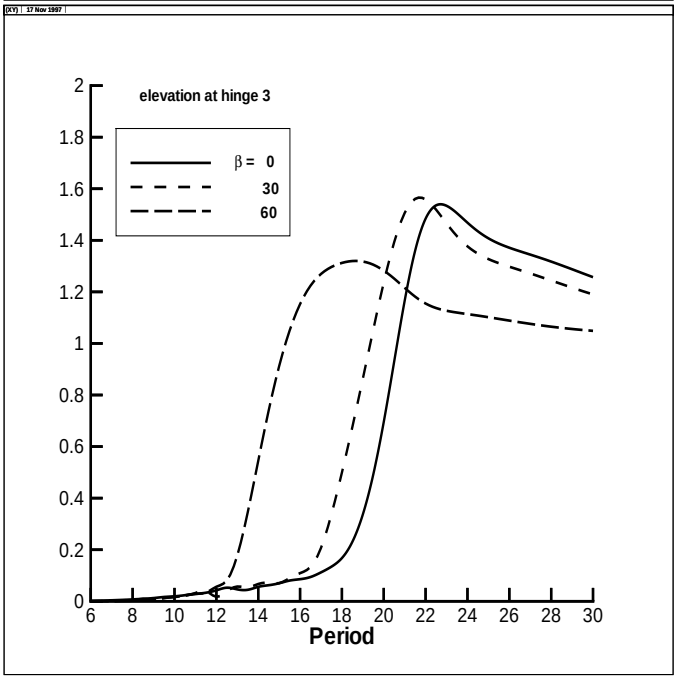

Figure 3: RAO's for hinge 2 and hinge 3.

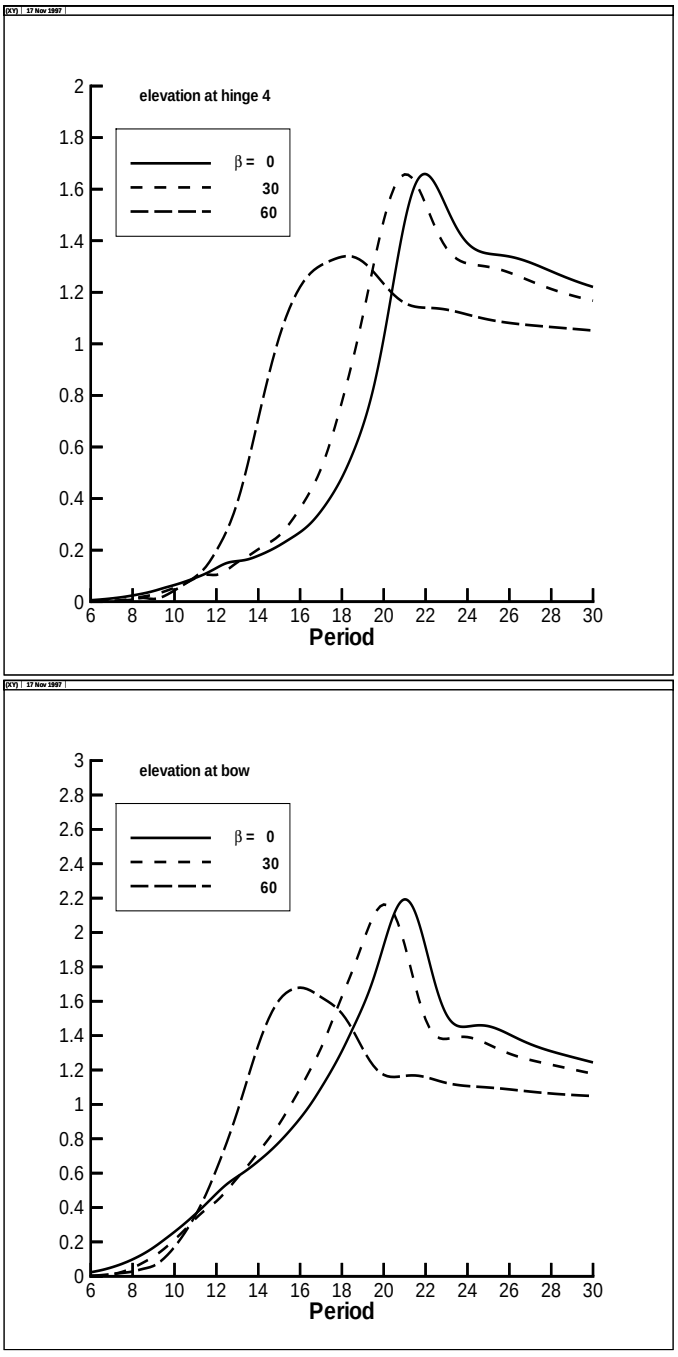

Figure 4: RAO's for hinge 4 and bow.